

1 **Modeling the transport of sodium dodecyl benzene sulfonate in riverine sediment**
2 **in the presence of multi-walled carbon nanotubes**

3

4 Biao Song^{a,b}, Piao Xu^{a,b}, Guangming Zeng^{a,b,*}, Jilai Gong^{a,b,*}, Xiaoxiao Wang^{a,b}, Jin Yan^{a,b},
5 Shengfan Wang^{a,b}, Peng Zhang^{a,b}, Weicheng Cao^{a,b}, Shujing Ye^{a,b}

6

7 ^a College of Environmental Science and Engineering, Hunan University, Changsha 410082,
8 P.R.China

9 ^b Key Laboratory of Environmental Biology and Pollution Control (Hunan University),
10 Ministry of Education, Changsha 410082, P.R.China

11

12 * Corresponding authors:

13 College of Environmental Science and Engineering, Hunan University, Changsha 410082,
14 P.R.China.

15 E-mail addresses: zgming@hnu.edu.cn (G. Zeng); jilaigong@gmail.com (J. Gong)

16

17 **Abstract**

18 The environmental risks of carbon nanotubes have received considerable
19 attention. In this work, the effects of multi-walled carbon nanotubes (MWCNTs) on
20 the adsorption of sodium dodecyl benzene sulfonate (SDBS) by riverine sediment and
21 the transport of SDBS in sediment were studied. MWCNTs could significantly
22 increase the adsorption capacity of the sediment for SDBS, thus affecting the
23 transport of SDBS in sediment. Maximum adsorption capacity of the sediment for
24 SDBS increases from 2.29 to 2.99 mg/g with the increasing content of MWCNTs
25 from 0% to 1.5%. Breakthrough curves (BTCs) of SDBS obtained from the column
26 experiments were described by the convection-dispersion equation, Thomas model,
27 and Yan model. The estimated retardation factor R increases with the incorporation of
28 MWCNTs, either in water or sediment. Additionally, the value of R is well correlated
29 to the content of MWCNTs in sediment. Compared with Thomas model, Yan model is
30 more suitable for fitting the BTCs with all the values of $R^2 \geq 0.951$, but it tends to
31 overestimate the maximum adsorption capacity when the content of MWCNTs in
32 sediment is relatively higher. The results of SDBS retention in sediment indicate that
33 MWCNTs can increase the accumulation of SDBS in the top sediment layer, while
34 they can impede the transport of SDBS into deeper sediment layer when incorporated
35 into the sediment. These effects should be taken into consideration for risk assessment
36 of CNTs in the aquatic environment.

37

38 **Keywords:** Adsorption; Transport; Sodium dodecyl benzene sulfonate; Multi-walled
39 carbon nanotubes; Sediment; Environmental risk

40

41

42 1. Introduction

43 Carbon nanotubes (CNTs), composed of carbon atoms in a periodic hexagonal
44 arrangement, are hollow cylinders with a diameter in the nanometer range.
45 Single-walled nanotubes (SWCNTs) and multi-walled nanotubes (MWCNTs) are two
46 main types of CNTs. Since their observation was first reported by Iijima in
47 1991(Iijima 1991), CNTs have been attracting much attention of researchers because
48 of their unique mechanical, thermal, optical, and electronic properties, as well as
49 many potential applications (Popov 2004, Zhang et al. 2007, Huang et al. 2008, Tang
50 et al. 2008, De Volder et al. 2013). Current production capacity of CNTs worldwide
51 has exceeded 5,000 tonnes per year, and is increasing with an annual growth rate of
52 32.5% (Patel 2011, De Volder et al. 2013). Increasing production and application of
53 CNTs will inevitably result in the release of these nanomaterials into the environment.
54 In a multimedia environment (atmosphere, soil, water, and sediment), mass
55 accumulation of CNTs was mostly in soil and sediment (Yang et al. 2010, Liu and
56 Cohen 2014). Based on the research of Koelmans et al. (2009), the estimated
57 concentrations of manufactured carbon-based nanoparticles in aquatic sediment are
58 ranging from 1.2 to 2000 micrograms per kilogram of the dry sediment. And it is
59 likely that the concentrations of CNTs in sediment will increase in the future.

60 CNTs have strong adsorption affinity for various organic and inorganic
61 contaminants (Gong et al. 2009, Song et al. 2017a, Song et al. 2017b). As sediment is
62 also the ultimate reservoir of various contaminants in aquatic ecosystem, the
63 interaction between CNTs and contaminants may alter the fate and transport of these

64 contaminants, significantly influencing their mobility, toxicity, and bioavailability (Xu
65 et al. 2012a, Zeng et al. 2013a, b, Cheng et al. 2016). For example, Sun et al. (2015)
66 found that CNTs released into sediment would increase the adsorption capacity of
67 Cd(II) by sediment. Fang et al. (2013) demonstrated that TX100 suspended MWCNTs
68 could facilitate the transport of phenanthrene in soil columns, while Li et al. (2013)
69 reported that 5 mg/g CNTs could significantly retain polycyclic aromatic
70 hydrocarbons in soil. Recent research by Liang et al. (2016) showed that CNTs could
71 enhance the mobility of tetrabromobisphenol A in saturated porous media. Zhang et al.
72 (2017) also observed facilitated transport of chlordecone and sulfadiazine in the
73 presence of CNTs in soil. However, studies investigating the effect of CNTs on the
74 transport of contaminants in real riverine sediment were insufficient.

75 Since sodium dodecyl benzene sulfonate (SDBS) is commonly used to increase
76 the dispersity and stability of CNTs in aqueous solutions, most of the current studies
77 focused on the effect of SDBS on the properties, transport, and fate of CNTs (Tian et
78 al. 2011, Ju et al. 2012, Wusiman et al. 2013). However, few studies investigated the
79 effect of CNTs on the transport and fate of SDBS. As an anionic surfactant, SDBS is
80 usually present in detergent, soap, as well as cosmetic, and widely used as emulsifier,
81 dispersant, lubricant, and preservative in industrial processes (Myers 2005, Taffarel
82 and Rubio 2010). Because of its extensive applications, a large amount of SDBS is
83 released into the aquatic environment, causing serious environmental problems. The
84 adverse effects of the surfactant on the aquatic environment and human health have
85 been studied and reported elsewhere. According to the available literature, SDBS

86 exhibits toxic effects towards algae, benthic invertebrates, fishes, and human cells (Qv
87 and Jiang 2013, Mu et al. 2014, Zhang et al. 2015, Zhang et al. 2016). Considering the
88 ecological and human health risks of SDBS, the environmental behavior of SDBS in
89 the presence of CNTs in the aquatic environment should be studied.

90 In this study, research on the transport of SDBS in riverine sediment in the
91 presence of MWCNTs was conducted. The objectives of the present study were (1) to
92 investigate the effect of MWCNTs on the adsorption of SDBS by sediment, and (2) to
93 study the transport of SDBS in the presence and absence of MWCNTs in riverine
94 sediment by column experiments and numerical modeling.

96 **2. Materials and methods**

98 *2.1. Chemicals, sediment, and carbon nanotubes*

99 SDBS ($C_{18}H_{29}NaO_3S$, AR) was purchased from Sinopharm Chemical Reagent
100 Co., Ltd., Shanghai, China. All other reagents in this study were of analytical grade or
101 better and commercially available. Surface sediment samples (0–15 cm) were
102 collected from Changsha section of the Xiangjiang River in Hunan Province, China.
103 Sediment samples were air-dried at room temperature and then crushed in a porcelain
104 mortar. Subsequently, the samples were sieved over a one mm mesh sieve and
105 homogenized prior to use. Sediment properties including pH, zeta potential, electrical
106 conductivity, organic carbon content, cation exchange capacity, and texture (sand, silt,
107 and clay) were measured with the methods mentioned in previous literature (Song et

108 al. 2017b). Industrial grade MWCNTs with an outer diameter of 10–20 nm and a
109 length of 5–10 μm were used in this study. They were purchased from Chengdu
110 Organic Chemistry Co., Chinese Academy of Sciences, Chengdu, China.

111

112 2.2. Batch adsorption experiments

113 Kinetics experiments of SDBS adsorption onto MWCNTs, sediment, and
114 sediment-MWCNTs mixtures (content of MWCNTs in sediment, w/w: 0.5%, 1.0%,
115 and 1.5%) were performed in 250 mL conical flasks containing 20 mg/L SDBS on a
116 shaker at 180 rpm, 25 ± 1 °C. Adsorbent dosage of MWCNTs was 0.3 g/L, while the
117 dosages of sediment, and sediment-MWCNTs were both 20 g/L. The samples were
118 taken out from the flask after predetermined time intervals (from 30 s to 300 min),
119 and the concentrations of SDBS were determined by high performance liquid
120 chromatography (HPLC, Agilent 1100, USA) equipped with UV-vis variable
121 wavelength detector (VWD) and reversed-phase C18 column. Methanol (90%, v/v)
122 was used as the mobile phase at a flow rate of 1 mL/min with constant detection
123 wavelength at 224 nm.

124 Adsorption isotherm experiments were conducted in conical flasks containing
125 SDBS solutions of different concentrations (from 10 to 80 mg/L) on a shaker at 180
126 rpm, 25 ± 1 °C. The dosages of adsorbents were the same as those in kinetics
127 experiments. After a 2 h equilibrium, samples were taken out and the concentrations
128 of SDBS were determined by the above-mentioned analytical method of HPLC.

129

130 2.3. Column experiments

131 Column transport experiments of SDBS in various sediment columns were
132 carried out under saturated flow conditions. A Teflon column with a length of 300 mm
133 and an inner diameter of 24 mm was used in the experiments. The column packing
134 was based on previously reported methods with appropriate modifications (Zhuang et
135 al. 2003, Tričković et al. 2016). Concretely, a stainless steel wire mesh with pore size
136 of 0.14 mm was placed at the bottom of the column, and then a quartz sand (25–50
137 mesh) layer of 10 mm was added for supporting the sediment particles. Subsequently,
138 ultrapure water was introduced into the column from the bottom to a certain height
139 with a peristaltic pump (DDB-300, Zhisun Equipment Co., Ltd., Shanghai, China).
140 After that, sediment was slowly poured into the column by 5–6 mm increments until
141 the column was packed to a height of 48 mm. During the packing process, the
142 sediment in the column was stirred with a glass rod to ensure homogeneous packing
143 and to avoid air entrapment. After the sediment column was prepared, a potassium
144 bromide (KBr) solution was used as a conservative tracer for characterizing the
145 sediment column and the hydraulic conditions.

146 Two sets of column transport experiment, denoted as Set I and Set II, were
147 conducted. In Set I, 50 mg/L SDBS, 50 mg/L SDBS containing 0.3 g/L MWCNTs
148 (reached adsorption equilibrium in advance), and 32 mg/L SDBS (an equilibrium
149 concentration of 50 mg/L SDBS containing 0.3 g/L MWCNTs) were pumped
150 respectively to the top of the sediment columns. For Set II, sediment in the column
151 was mixed with MWCNTs, and the contents of MWCNTs were 0.5%, 1.0%, and 1.5%

152 (w/w), respectively. In this set, 50 mg/L SDBS solutions were pumped to the columns
153 by peristaltic pump and transported from the top down. The duration of each column
154 transport experiment was 24 h for both Set I and Set II. During the column
155 experiments, a constant water head of 150 mm was maintained and the effluent was
156 collected at regular intervals for the measurement of SDBS concentrations.

157 At the end of the column experiment, sediment in the column was air-dried and
158 equally divided into 6 segments. Then SDBS concentrations in these segments were
159 analyzed based on previously reported method (Santos et al. 2007). In short, SDBS in
160 the sediment was extracted with methanol. For each extraction, 20 mL methanol was
161 added into the beaker containing the sediment, followed by shaking the beaker on a
162 shaker for 5 min. Afterwards, the sample was sonicated for 30 min and then
163 centrifuged to collect the supernatants. After filtered through 0.45 μm filter membrane,
164 the SDBS concentration in the filtrate was determined by HPLC.

166 2.4. Numerical modeling

167 The obtained data of adsorption kinetics were fitted with pseudo-first-order
168 kinetic model and pseudo-second-order kinetic model. The models are given by the
169 following equations (Hu et al. 2011, Xu et al. 2012b):

$$170 \ln(q_e - q_t) = \ln q_e - k_1 t \quad (\text{Pseudo-first-order kinetic model}) \quad (1)$$

$$171 \frac{t}{q_t} = \frac{1}{k_2 q_e^2} + \frac{t}{q_e} \quad (\text{Pseudo-second-order kinetic model}) \quad (2)$$

172 where q_e and q_t (mg/g) are the amount of adsorbed SDBS at equilibrium and time t
173 (min), k_1 and k_2 are the first-order rate constant (1/min) and second-order rate constant

174 (g/(mg min)), respectively.

175 Experimental results of the adsorption isotherms were described by Langmuir
176 and Freundlich models, which are represented by the following equations (Hu et al.
177 2011, Xu et al. 2012b):

$$178 \quad q_e = \frac{q_m K_L c_e}{1 + K_L c_e} \quad (\text{Langmuir model}) \quad (3)$$

$$179 \quad q_e = K_F c_e^{\frac{1}{n}} \quad (\text{Freundlich model}) \quad (4)$$

180 where q_e (mg/g) is the amount of adsorbed SDBS at equilibrium, q_m (mg/g) is the
181 maximum adsorption capacity, K_L (L/mg) is the Langmuir constant, c_e (mg/L) is the
182 equilibrium concentration of SDBS, K_F (mg/g(mg/L)^{-1/n}) and n (dimensionless) are
183 Freundlich constants.

184 Breakthrough curves (BTCs) are used to indicate the transport of SDBS through
185 sediment columns. Under the condition of steady flow, the BTCs can be described by
186 the convection-dispersion equation (CDE). BTC of the tracer (Br^-) is fitted with
187 deterministic equilibrium CDE (Toride et al. 1995), which is written as

$$188 \quad R \frac{\partial c}{\partial t} = D \frac{\partial^2 c}{\partial x^2} - v \frac{\partial c}{\partial x} \quad (5)$$

189 where c (mg/L) is the Br^- concentration in effluent, R (dimensionless) is the
190 retardation factor, D (cm²/h) is the dispersion coefficient, v (cm/h) is the average pore
191 water velocity, x (cm) is distance, and t (h) is time. Based on the assumption that Br^-
192 is nonreactive and can not be adsorbed onto sediment ($R = 1$), the estimated D and v
193 by the equilibrium CDE are 3.35 cm²/h and 4.73 cm/h (Fig. 2a, $R^2 = 0.982$),
194 respectively. These parameters are then used for understanding the dominant process

195 that impact the solute transport and analyzing the BTCs of SDBS transport.

196 The transport of SDBS in sediment can be described by a two-site chemical
197 nonequilibrium model (TSM, a deterministic nonequilibrium CDE model), in which
198 adsorption sites of the sediment are divided into two types: equilibrium adsorption
199 sites and kinetic adsorption sites (Toride et al. 1995). Dimensionless form of the TSM
200 is given by

$$201 \quad \beta R \frac{\partial C_1}{\partial T} = \frac{1}{P} \frac{\partial^2 C_1}{\partial Z^2} - \frac{\partial C_1}{\partial Z} - \omega(C_1 - C_2) \quad (6)$$

$$202 \quad (1 - \beta)R \frac{\partial C_2}{\partial T} = \omega(C_1 - C_2) \quad (7)$$

$$203 \quad \beta = \frac{\theta + fK_d}{\theta + K_d} \quad (8)$$

$$204 \quad \omega = \frac{\alpha(1 - \beta)RL}{v} \quad (9)$$

$$205 \quad R = 1 + \frac{\rho_b K_d}{\theta} \quad (10)$$

$$206 \quad T = \frac{vt}{L} \quad (11)$$

$$207 \quad P = \frac{vL}{D} \quad (12)$$

$$208 \quad Z = \frac{x}{L} \quad (13)$$

209 where β is a partitioning coefficient of equilibrium and kinetic adsorption sites, C is
210 dimensionless concentration, T is dimensionless time, P is Peclet number, Z is
211 dimensionless distance, ω is a dimensionless mass transfer coefficient, L (cm)
212 represents a characteristic length, θ is volumetric water content, f is the fraction of
213 exchange sites assumed to be at equilibrium, K_d is the distribution coefficient for
214 linear adsorption, α is a first-order kinetic rate coefficient, ρ_b is the bulk density of
215 sediment, and the subscripts 1 and 2 refer to equilibrium and kinetic adsorption sites,

216 respectively. Other symbols have the same meaning as those in Eq. (5). When fitting
 217 the BTCs of SDBS, the parameter D and ν are fixed as the value obtained by the
 218 equilibrium CDE, and then the transport parameter R , β , and ω are estimated with
 219 TSM.

220 Thomas and Yan models are widely used for describing the adsorption process in
 221 a continuous system (Valizadeh et al. 2016). In this study, they are applied for
 222 modeling the BTCs concerning SDBS adsorption. The models are given by the
 223 following equations:

$$224 \quad \frac{c}{c_0} = \frac{1}{1 + \exp\left(\frac{K_T q_T m}{Q} - K_T c_0 t\right)} \quad (\text{Thomas model}) \quad (14)$$

$$225 \quad \frac{c}{c_0} = 1 - \frac{1}{1 + \left(\frac{Q^2 t}{K_Y q_Y m}\right)^{\left(\frac{K_Y c_0}{Q}\right)}} \quad (\text{Yan model}) \quad (15)$$

226 where c (mg/L) is the SDBS concentration in effluent, c_0 (mg/L) is the SDBS
 227 concentration in influent, K_T (h/h/mg) is the Thomas rate constant, K_Y (L/h/mg) is the
 228 Yan rate constant, m (g) is the mass of adsorbent, Q (L/h) is the influent flow rate, t (h)
 229 is time, and q_T (mg/g) and q_Y (mg/g) are the maximum adsorption capacity estimated
 230 by Thomas model and Yan model, respectively. Yan model is an empirical formula
 231 that overcomes some deficiencies of Thomas model, especially that of the prediction
 232 of solute concentration in effluent near time zero.

233 OriginPro 9.1 software (OriginLab Corporation, Massachusetts, USA) was used
 234 to fit the adsorption models and BTC models concerning SDBS adsorption. Fitting of
 235 BTC models concerning transport parameters was performed with the program

236 CXTFIT 2.0 executed in the software STANMOD (version 2.08) (Toride et al. 1995,
237 Simunek et al. 1999).

238

239 **3. Results and discussion**

240

241 *3.1. Characterization of the sediment and MWCNTs*

242 The measured pH value, organic carbon content, cation exchange capacity, zeta
243 potential, and electrical conductivity of the sediment are 7.92, 1.63%, 10.8 cmol/kg,
244 -18.4 mV, and 0.144 mS/cm, respectively. Additionally, the sediment sample has a
245 composition of 23.4% sand, 27.6% silt, and 49.0% clay. MWCNTs used in this study
246 were characterized by scanning electron microscope (SEM) and specific surface
247 analyzer. Typical tubular structure of the MWCNTs was observed with SEM images
248 shown in Fig. S1. According to the specific surface analysis, Brunauer-Emmett-Teller
249 (BET) specific surface area of the MWCNTs is 134 m²/g.

250

251 *3.2. Effect of MWCNTs on the adsorption of SDBS by sediment*

252 The MWCNTs significantly influenced the adsorption of SDBS by sediment. As
253 shown in Fig. 1, the adsorption amount of SDBS increases with the increase of time.
254 The whole process of adsorption can be broadly divided onto three stages. During the
255 first stage (the first 20 min), a rapid increase of the adsorption amount of SDBS is
256 observed as a result of the high concentration gradient. In the second stage (20–50
257 min), the adsorption amount increases slowly until the arrival of the last stage (>50

258 min). The maximum adsorption amount is reached at the last stage, and the adsorption
259 gets to an equilibrium state. Compared with the adsorption by sediment, the
260 adsorption amount of SDBS by MWCNTs increases more quickly in the first stage.

261 Parameters of the fitted models for SDBS adsorption are listed in Table S1 and
262 Table S2. It can be found that experimental data of adsorption kinetics are better fitted
263 by pseudo-second-order kinetic model ($R^2 \geq 0.911$) than pseudo-first-order kinetic
264 model ($R^2 \geq 0.828$). Such result indicates that rate-limiting step of the adsorption
265 processes is a chemical adsorption in which valence forces generated by exchanging
266 or sharing electrons are involved (Fan et al. 2008, Feng et al. 2010, Xu et al. 2012b).
267 Langmuir and Freundlich models could be well used to fit the isotherm data with all
268 the values of $R^2 \geq 0.926$. The estimated q_m of MWCNTs for SDBS adsorption is 115
269 mg/g, which is much more than that of sediment (2.29 mg/g). This could be due to the
270 specific molecular structure of SDBS. On the one hand, the strong π - π
271 electron-donor-acceptor interaction between the benzene ring of SDBS molecule and
272 the highly polarizable graphene sheets of MWCNTs can facilitate the adsorption
273 processes (Lin et al. 2015). On the other hand, the hydrophobic tail (12-carbon alkyl
274 chain) of SDBS may be bound to the surface of MWCNTs through hydrophobic
275 attraction (Lin et al. 2010). Additionally, the values of q_m (from 2.29 to 2.99 mg/g)
276 and K_F (from 0.0713 to 0.844 mg/g (mg/L)^{-1/n}) increase with the increasing content of
277 MWCNTs in sediment (from 0% to 1.5%), implying that the adsorption capacity of
278 sediment for SDBS was enhanced as a result of the incorporation of MWCNTs.

279

280 3.3. *Effect of MWCNTs on the transport of SDBS in sediment*

281

282 3.3.1. Analysis and modeling of the BTCs concerning transport parameters

283 The experimental and CDE fitting results of SDBS transport through sediment
284 columns in Set I and Set II are shown in Fig. 2, and associated parameters estimated
285 by the model are listed in Table 1. It is observed from the table that the experimental
286 data are well fitted by TSM with all the values of $R^2 \geq 0.927$. However, the
287 equilibrium CDE is not suitable for describing the BTCs of SDBS (data not shown).
288 Retardation factor R is a derived parameter to quantify the slowing down of solute
289 transport. In the experimental results of Set I, a lower value of R (5.10) is obtained
290 with an initial SDBS concentration of 50 mg/L, while the value of R increases to 5.62
291 with an initial SDBS concentration of 32 mg/L. Thus, it can be regarded that a slightly
292 higher concentration of SDBS is able to overcome part of the mass transfer resistance,
293 resulting in a lower value of R . Similar results can be found in previous literature
294 (Fonseca et al. 2009, Florido et al. 2010). Considering the surfactant characteristic of
295 SDBS, the effect of the critical micelle concentration (CMC) on the transport of
296 SDBS were investigated (Fig. S2). We determined the CMC of SDBS through
297 conductivity measurement, and the result is 1.72 mmol/L (599.16 mg/L). Thus, SDBS
298 aqueous solutions with three different concentrations (200, 600, and 1000 mg/L) were
299 used and transported through the sediment columns. Compared with 32 and 50 mg/L
300 SDBS, higher SDBS concentration near CMC leads to an increase in R value (> 5.62),
301 and the value decreases with the increasing SDBS concentration (11.3, 7.00, and 5.91).
302 When SDBS concentration increases but is below the CMC, the surfactant may

303 increase the dispersion of colloidal-size sediment particles, leading to sediment pore
304 clogging. And when the concentration up to the CMC, clay-size sediment particles
305 can be trapped in the SDBS micelles and cannot settle out of the solution (Abdul et al.
306 1990). Using 50 mg/L SDBS containing 0.3 g/L MWCNTs as the influent
307 significantly increases calculated R to 37.0 ($c_0 = 50$ mg/L). This is mainly because of
308 the strong adsorption affinity of MWCNTs towards SDBS.

309 Partitioning coefficient β and mass transfer coefficient ω can be used for
310 evaluating the validity of equilibrium assumption for the transport conditions (Pang
311 and Close 1999). When $\beta = 1$, the transport is under an equilibrium condition and all
312 the adsorption sites are instantaneous. When $0 < \beta < 1$, a nonequilibrium condition
313 exists and there are some rate-limited adsorption sites. A higher value of ω
314 corresponds to faster adsorption of the solute during transport process, and when $\omega \geq$
315 100, the transport is considered to be under an equilibrium condition (Pang and Close
316 1999). The calculated values of β for Set I (Table 1) indicated that more than 80% of
317 the adsorption sites were rate-limited and less than 10% of the adsorption sites were
318 instantaneous. The lower values of β ($\beta < 0.196$) and ω ($\omega < 9.53$) in the experiment
319 results of Set I provide evidence for the nonequilibrium transport of SDBS in the
320 sediment columns. Additionally, it is interesting that the calculated R , β , and ω for the
321 influent with 50 mg/L SDBS containing 0.3 g/L MWCNTs ($c_0 = 32$ mg/L) are very
322 similar to those obtained with 32 mg/L SDBS as influent when using the equilibrium
323 concentration as initial concentration for modeling. We assume that the SDBS in the
324 influent can be divided into an adsorbed part and a free part. Based on the above

325 result, only the free part participated in the transport, while the adsorbed part
326 deposited with MWCNTs on the top of the sediment column. The result also shows
327 that the adsorption affinity between SDBS and MWCNTs is relatively stronger and
328 SDBS is not easy to be desorbed from MWCNTs under natural conditions.

329 In the results of Set II in Table 1, retardation factor increases (from 5.10 to 92.6)
330 with the increasing content of MWCNTs in sediment (from 0% to 1.5%). This is
331 mainly because of the strong adsorption affinity of MWCNTs for SDBS. After the
332 incorporation of MWCNTs into sediment, there is a consequential increase in the
333 resistance of SDBS transport through the sediment columns. Retardation factor can
334 also be estimated using Eq. (10) based on the batch adsorption experiments (Zhang et
335 al. 2011). The calculated values of R are 39.66, 70.44, 106.5, and 182.2, which
336 correspond to the MWCNTs content in sediment of 0%, 0.5%, 1.0%, and 1.5%,
337 respectively (Table S3). It is found that the R values determined through the batch
338 adsorption experiments are higher than those determined from the column
339 experiments. Nonetheless, the changing trends are consistent. The difference could be
340 due to a shorter retention time in column experiments (Pang and Close 1999).

341

342 3.3.2. Analysis and modeling of the BTCs concerning SDBS adsorption

343 Results of analysis and modeling of the BTCs concerning SDBS adsorption are
344 shown in Fig. 3 and Table 2. Thomas model can well fit most BTCs except that using
345 the influent of 50 mg/L SDBS containing 0.3 g/L MWCNTs and modeling with 50
346 mg/L as the initial concentration ($R^2 = 0.752$). Compared with Thomas model, Yan

347 model is more suitable for fitting the BTCs with all the values of $R^2 \geq 0.951$. In the
348 experiment results of Set I, q_T and q_Y increase with the incorporation of MWCNTs in
349 influent, while the rate constant K_T and K_Y vary inversely. For the influent with 50
350 mg/L SDBS containing 0.3 g/L MWCNTs ($c_0 = 32$ mg/L), the modeling results are
351 also similar to those obtained with 32 mg/L SDBS as influent, which further confirms
352 the foregoing conclusion. For Set II, 50 mg/L SDBS can completely ($c/c_0 = 1$) break
353 through the sediment column without MWCNTs in about 12 hours, after which the
354 concentration of SDBS in effluent reaches a stationary value of 50 mg/L. When
355 MWCNTs were incorporated into the sediment, the transport of SDBS in sediment
356 column was much slower. For sediment columns incorporated with 0.5%, 1.0%, and
357 1.5% MWCNTs, the values of c/c_0 are calculated to be 0.66, 0.25, and 0.09 after 24
358 hours, respectively (Fig. 3b). A higher content of MWCNTs in sediment leads to
359 higher values of q_T and q_Y . Most values of maximum adsorption capacity estimated
360 by Thomas model and Yan model (Table 2) are lower than those obtained from batch
361 adsorption tests (Table S2) because of a shorter retention time. However, when the
362 content of MWCNTs in sediment increase to 1.5%, the value of q_Y is estimated to be
363 9.96 mg/g, which is much higher than that (2.99 mg/g) obtained from the batch
364 adsorption tests. The result suggests that Yan model tends to overestimate the
365 maximum adsorption capacity when the content of MWCNTs in sediment is relatively
366 higher. The rate constant K_T and K_Y , which characterize the rate of SDBS transfer
367 from the liquid to sediment, decrease with the increase in content of MWCNTs in
368 sediment. The lower values of rate constants indicate a greater decrease of the

369 adsorption rate with the increase of time due to fewer unoccupied adsorption sites
370 (Shahbazi et al. 2011).

371

372 3.3.3. Retention of SDBS in sediment

373 MWCNTs have a remarkable influence on the retention of SDBS in sediment
374 (Fig. 4). Under natural conditions, SDBS can be intercepted during the transport
375 process due to mechanical resistance, adsorption, complexation, gravity sedimentation,
376 etc. For influent with 50 mg/L SDBS, the final concentrations of SDBS in sediment
377 segments from the top to the bottom are 0.39, 0.37, 0.37, 0.36, 0.27, 0.22 mg/g,
378 respectively (Fig. 4a). For influent with 32 mg/L SDBS, the concentrations of SDBS
379 in corresponding sediment segments decrease slightly. For example, SDBS
380 concentrations of the top and the bottom segments are 0.35 and 0.19 mg/g,
381 respectively. When MWCNTs were incorporated into the influent, transport of SDBS
382 through the sediment column became more difficult. The adsorbed SDBS deposited
383 with MWCNTs on the top of the sediment column, resulting in a high concentration
384 of SDBS (1.96 mg/g) in the top sediment segment. For Set II, the concentrations of
385 SDBS in the top segments are 0.39, 0.62, 0.82, and 1.10 mg/g, while those in the
386 bottom segments are 0.22, 0.13, 0.09, and 0.07 mg/g when the contents of MWCNTs
387 in sediment columns are 0%, 0.5%, 1.0%, and 1.5%, respectively (Fig. 4b). These
388 results indicate that MWCNTs can increase the accumulation of SDBS in the top
389 sediment layer, either in water or sediment. On the other hand, MWCNTs in sediment
390 can impede the transport of SDBS into deeper sediment layer. This is mainly because

391 of strong adsorption affinity of MWCNTs for SDBS and low mobility of MWCNTs in
392 riverine sediment.

393 Nevertheless, some previous studies reported the facilitated transport of
394 contaminants in the presence of MWCNTs (Fang et al. 2013, Zhang et al. 2017). The
395 different results can be attributed to that the MWCNTs were pretreated before the
396 column experiments and the size of particles in porous media was relatively larger in
397 these studies. As a result, MWCNTs showed high mobility in these porous media,
398 leading to the co-transport of contaminants with MWCNTs. In our study, the
399 MWCNTs used in the experiments showed no macroscopic transport in the riverine
400 sediment, thus they impeded the transport of SDBS in sediment due to the increase of
401 adsorption capacity of the sediment incorporated with MWCNTs.

403 3.4. Environmental implications

404 The release of CNTs into sediment can significantly influence the adsorption
405 behaviors of SDBS by sediment and the transport of SDBS in sediment. The q_m , q_T ,
406 q_Y , R estimated from the column experiments and the batch adsorption experiments,
407 and retention amount of SDBS in sediment increased after the incorporation of CNTs.
408 Relationships between the content of MWCNTs in sediment and these parameters
409 were analyzed. The Pearson's correlation coefficients were calculated to be 0.957,
410 0.992, 0.975, 0.997, 0.860, and 0.990, respectively (Table S4). The results indicate a
411 concentration-dependent effect of MWCNTs on SDBS transport in riverine sediment.
412 Retardation factors estimated by the column experiments can be interpreted as the

413 transport distance of SDBS in sediment, since R is also expressed as the ratio of the
414 velocity of pore water to that of solute (Baik and Lee 1994). In other words, for
415 example, when the pore water flows for a distance of 92.6 cm in the sediment
416 incorporated with 1.5% MWCNTs, SDBS can only be transported for one centimeter
417 ($R = 92.6$). Although the ecological risks of CNTs are not fully understood, the
418 retention of SDBS may increase the ecotoxicity of CNTs to the aquatic organisms due
419 to the toxicity of SDBS and the prolonged contact time.

420

421 **4. Conclusions**

422 In this work, the effects of MWCNTs on the adsorption and transport of SDBS in
423 riverine sediment were investigated. The main conclusions are as follows:

- 424 • MWCNTs significantly increase the adsorption capacity of the sediment for
425 SDBS, thus affecting the transport of SDBS in sediment.
- 426 • The retardation factor R estimated by the CDE model increases with the
427 incorporation of MWCNTs, either in water or sediment. Additionally, the value of
428 R is well correlated to the content of MWCNTs in sediment.
- 429 • Compared with Thomas model, Yan model is more suitable for fitting the BTCs
430 with all the values of $R^2 \geq 0.951$, but it tends to overestimate the maximum
431 adsorption capacity when the content of MWCNTs in sediment is relatively
432 higher.
- 433 • MWCNTs can increase the accumulation of SDBS in the top sediment layer,
434 while they can impede the transport of SDBS into deeper sediment layer when
435 incorporated into the sediment. Further studies on the potential ecological impacts

436 of CNTs and their mechanisms should be conducted.

437

438

439

440 **Acknowledgements**

441 This work was supported by National Natural Science Foundation of China
442 (51521006, 51579095, 51378190), the Program for Changjiang Scholars and
443 Innovative Research Team in University (IRT-13R17), Hunan province university
444 innovation platform open fund project (14K020) and the Interdisciplinary Research
445 Funds for Hunan University.

446

Accepted Manuscript

447 **References**

448 Abdul, A.S., Gibson, T.L. and Rai, D.N. (1990) Selection of Surfactants for the
449 Removal of Petroleum Products from Shallow Sandy Aquifers. *Ground Water* 28(6),
450 920-926.

451 Baik, M.H. and Lee, K.J. (1994) Transport of radioactive solutes in the presence of
452 chelating agents. *Annals of Nuclear Energy* 21(2), 81-96.

453 Cheng, Y., He, H., Yang, C., Zeng, G., Li, X., Chen, H. and Yu, G. (2016) Challenges
454 and solutions for biofiltration of hydrophobic volatile organic compounds.
455 *Biotechnology Advances* 34(6), 1091-1102.

456 De Volder, M.F.L., Tawfick, S.H., Baughman, R.H. and Hart, A.J. (2013) Carbon
457 nanotubes: Present and future commercial applications. *Science* 339(6119), 535-539.

458 Fan, T., Liu, Y., Feng, B., Zeng, G., Yang, C., Zhou, M., Zhou, H., Tan, Z. and Wang,
459 X. (2008) Biosorption of cadmium(II), zinc(II) and lead(II) by *Penicillium*
460 *simplicissimum*: Isotherms, kinetics and thermodynamics. *Journal of Hazardous*
461 *Materials* 160(2), 655-661.

462 Fang, J., Shan, X., Wen, B. and Huang, R. (2013) Mobility of TX100 suspended
463 multiwalled carbon nanotubes (MWCNTs) and the facilitated transport of
464 phenanthrene in real soil columns. *Geoderma* 207-208, 1-7.

465 Feng, Y., Gong, J.L., Zeng, G.M., Niu, Q.Y., Zhang, H.Y., Niu, C.G., Deng, J.H. and
466 Yan, M. (2010) Adsorption of Cd (II) and Zn (II) from aqueous solutions using
467 magnetic hydroxyapatite nanoparticles as adsorbents. *Chemical Engineering Journal*
468 162(2), 487-494.

469 Florido, A., Valderrama, C., Arévalo, J.A., Casas, I., Martínez, M. and Miralles, N.
470 (2010) Application of two sites non-equilibrium sorption model for the removal of
471 Cu(II) onto grape stalk wastes in a fixed-bed column. Chemical Engineering Journal
472 156(2), 298-304.

473 Fonseca, B., Teixeira, A., Figueiredo, H. and Tavares, T. (2009) Modelling of the
474 Cr(VI) transport in typical soils of the North of Portugal. Journal of Hazardous
475 Materials 167(1-3), 756-762.

476 Gong, J.L., Wang, B., Zeng, G.M., Yang, C.P., Niu, C.G., Niu, Q.Y., Zhou, W.J. and
477 Liang, Y. (2009) Removal of cationic dyes from aqueous solution using magnetic
478 multi-wall carbon nanotube nanocomposite as adsorbent. Journal of Hazardous
479 Materials 164(2), 1517-1522.

480 Hu, X., Wang, J., Liu, Y., Li, X., Zeng, G., Bao, Z., Zeng, X., Chen, A. and Long, F.
481 (2011) Adsorption of chromium (VI) by ethylenediamine-modified cross-linked
482 magnetic chitosan resin: Isotherms, kinetics and thermodynamics. Journal of
483 Hazardous Materials 185(1), 306-314.

484 Huang, D.L., Zeng, G.M., Feng, C.L., Hu, S., Jiang, X.Y., Tang, L., Su, F.F., Zhang, Y.,
485 Zeng, W. and Liu, H.L. (2008) Degradation of lead-contaminated lignocellulosic
486 waste by *Phanerochaete chrysosporium* and the reduction of lead toxicity.
487 Environmental Science & Technology 42(13), 4946-4951.

488 Iijima, S. (1991) Helical microtubules of graphitic carbon. Nature 354(6348), 56-58.

489 Ju, L., Zhang, W., Wang, X., Hu, J. and Zhang, Y. (2012) Aggregation kinetics of
490 SDBS-dispersed carbon nanotubes in different aqueous suspensions. Colloids and

491 Surfaces A: Physicochemical and Engineering Aspects 409, 159-166.

492 Koelmans, A.A., Nowack, B. and Wiesner, M.R. (2009) Comparison of manufactured
493 and black carbon nanoparticle concentrations in aquatic sediments. Environmental
494 Pollution 157(4), 1110-1116.

495 Li, S., Turaga, U., Shrestha, B., Anderson, T.A., Ramkumar, S.S., Green, M.J., Das, S.
496 and Cañas-Carrell, J.E. (2013) Mobility of polyaromatic hydrocarbons (PAHs) in soil
497 in the presence of carbon nanotubes. Ecotoxicology and Environmental Safety 96,
498 168-174.

499 Liang, L., Ju, L., Hu, J., Zhang, W. and Wang, X. (2016) Transport of sodium
500 dodecylbenzene sulfonate (SDBS)-dispersed carbon nanotubes and enhanced mobility
501 of tetrabromobisphenol A (TBBPA) in saturated porous media. Colloids and Surfaces
502 A: Physicochemical and Engineering Aspects 497, 205-213.

503 Lin, D., Liu, N., Yang, K., Xing, B. and Wu, F. (2010) Different stabilities of
504 multiwalled carbon nanotubes in fresh surface water samples. Environmental
505 Pollution 158(5), 1270-1274.

506 Lin, L., Peng, H. and Ding, G. (2015) Dispersion stability of multi-walled carbon
507 nanotubes in refrigerant with addition of surfactant. Applied Thermal Engineering 91,
508 163-171.

509 Liu, H.H. and Cohen, Y. (2014) Multimedia environmental distribution of engineered
510 nanomaterials. Environmental Science & Technology 48(6), 3281-3292.

511 Mu, Z., Liu, X., Zhao, Y. and Zhang, J. (2014) Cytotoxic effects of sodium dodecyl
512 benzene sulfonate on human keratinocytes are not associated with proinflammatory

513 cytokines expression. Chinese medical journal 127(21), 3777-3781.

514 Myers, D. (2005) Surfactant science and technology, John Wiley & Sons, Inc.,
515 Hoboken, New Jersey.

516 Pang, L. and Close, M.E. (1999) Non-equilibrium transport of Cd in alluvial gravels.
517 Journal of Contaminant Hydrology 36(1–2), 185-206.

518 Patel, V. (2011) Global carbon nanotubes market: Industry beckons. Nanotech
519 Insights 2(3), 31-35.

520 Popov, V.N. (2004) Carbon nanotubes: properties and application. Materials Science
521 and Engineering: R: Reports 43(3), 61-102.

522 Qv, X.Y. and Jiang, J.G. (2013) Toxicity evaluation of two typical surfactants to
523 *Dunaliella bardawil*, an environmentally tolerant alga. Environmental Toxicology and
524 Chemistry 32(2), 426-433.

525 Santos, J.L., Aparicio, I. and Alonso, E. (2007) A new method for the routine analysis
526 of LAS and PAH in sewage sludge by simultaneous sonication-assisted extraction
527 prior to liquid chromatographic determination. Analytica Chimica Acta 605(1),
528 102-109.

529 Shahbazi, A., Younesi, H. and Badiei, A. (2011) Functionalized SBA-15 mesoporous
530 silica by melamine-based dendrimer amines for adsorptive characteristics of Pb(II),
531 Cu(II) and Cd(II) heavy metal ions in batch and fixed bed column. Chemical
532 Engineering Journal 168(2), 505-518.

533 Simunek, J., Van Genuchten, M.T., Sejna, M., Toride, N. and Leij, F. (1999) The
534 STANMOD computer software for evaluating solute transport in porous media using

535 analytical solutions of convection-dispersion equation, Versions 1.0 and 2.0, U.S.
536 Salinity Laboratory, USDA, ARS, Riverside, California.

537 Song, B., Zeng, G., Gong, J., Liang, J., Xu, P., Liu, Z., Zhang, Y., Zhang, C., Cheng,
538 M., Liu, Y., Ye, S., Yi, H. and Ren, X. (2017a) Evaluation methods for assessing
539 effectiveness of in situ remediation of soil and sediment contaminated with organic
540 pollutants and heavy metals. *Environment International* 105, 43-55.

541 Song, B., Zeng, G., Gong, J., Zhang, P., Deng, J., Deng, C., Yan, J., Xu, P., Lai, C.,
542 Zhang, C. and Cheng, M. (2017b) Effect of multi-walled carbon nanotubes on
543 phytotoxicity of sediments contaminated by phenanthrene and cadmium.
544 *Chemosphere* 172, 449-458.

545 Sun, W., Jiang, B., Wang, F. and Xu, N. (2015) Effect of carbon nanotubes on Cd(II)
546 adsorption by sediments. *Chemical Engineering Journal* 264, 645-653.

547 Taffarel, S.R. and Rubio, J. (2010) Adsorption of sodium dodecyl benzene sulfonate
548 from aqueous solution using a modified natural zeolite with CTAB. *Minerals*
549 *Engineering* 23(10), 771-779.

550 Tang, L., Zeng, G.M., Shen, G.L., Li, Y.P., Zhang, Y. and Huang, D.L. (2008) Rapid
551 detection of picloram in agricultural field samples using a disposable
552 immunomembrane-based electrochemical sensor. *Environmental Science &*
553 *Technology* 42(4), 1207-1212.

554 Tian, Y., Gao, B. and Ziegler, K.J. (2011) High mobility of SDBS-dispersed
555 single-walled carbon nanotubes in saturated and unsaturated porous media. *Journal of*
556 *Hazardous Materials* 186(2-3), 1766-1772.

557 Toride, N., Leij, F. and Van Genuchten, M.T. (1995) The CXTFIT code for estimating
558 transport parameters from laboratory or field tracer experiments, U.S. Salinity
559 Laboratory, USDA, ARS, Riverside, California.

560 Tričković, J., Isakovski, M.K., Watson, M., Maletić, S., Rončević, S., Dalmacija, B.,
561 Kónya, Z. and Kukovecz, Á. (2016) Sorption behaviour of trichlorobenzenes and
562 polycyclic aromatic hydrocarbons in the absence or presence of carbon nanotubes in
563 the aquatic environment. *Water, Air, & Soil Pollution* 227(10), 1-16.

564 Valizadeh, S., Younesi, H. and Bahramifar, N. (2016) Highly mesoporous K_2CO_3 and
565 KOH/activated carbon for SDBS removal from water samples: Batch and fixed-bed
566 column adsorption process. *Environmental Nanotechnology, Monitoring &*
567 *Management* 6, 1-13.

568 Wusiman, K., Jeong, H., Tulugan, K., Affianto, H. and Chung, H. (2013) Thermal
569 performance of multi-walled carbon nanotubes (MWCNTs) in aqueous suspensions
570 with surfactants SDBS and SDS. *International Communications in Heat and Mass*
571 *Transfer* 41, 28-33.

572 Xu, P., Zeng, G.M., Huang, D.L., Feng, C.L., Hu, S., Zhao, M.H., Lai, C., Wei, Z.,
573 Huang, C., Xie, G.X. and Liu, Z.F. (2012a) Use of iron oxide nanomaterials in
574 wastewater treatment: A review. *Science of the Total Environment* 424, 1-10.

575 Xu, P., Zeng, G.M., Huang, D.L., Lai, C., Zhao, M.H., Wei, Z., Li, N.J., Huang, C. and
576 Xie, G.X. (2012b) Adsorption of Pb(II) by iron oxide nanoparticles immobilized
577 *Phanerochaete chrysosporium*: Equilibrium, kinetic, thermodynamic and mechanisms
578 analysis. *Chemical Engineering Journal* 203, 423-431.

579 Yang, C., Chen, H., Zeng, G., Yu, G. and Luo, S. (2010) Biomass accumulation and
580 control strategies in gas biofiltration. *Biotechnology Advances* 28(4), 531-540.

581 Zeng, G., Chen, M. and Zeng, Z. (2013a) Risks of neonicotinoid pesticides. *Science*
582 340(6139), 1403.

583 Zeng, G., Chen, M. and Zeng, Z. (2013b) Shale gas: Surface water also at risk. *Nature*
584 499(7457), 154.

585 Zhang, L., Wang, L., Zhang, P., Kan, A.T., Chen, W. and Tomson, M.B. (2011)
586 Facilitated transport of 2,2',5,5'-polychlorinated biphenyl and phenanthrene by
587 fullerene nanoparticles through sandy soil columns. *Environmental Science &*
588 *Technology* 45(4), 1341-1348.

589 Zhang, M., Engelhardt, I., Šimůnek, J., Bradford, S.A., Kasel, D., Berns, A.E.,
590 Vereecken, H. and Klumpp, E. (2017) Co-transport of chlordecone and sulfadiazine in
591 the presence of functionalized multi-walled carbon nanotubes in soils. *Environmental*
592 *Pollution* 221, 470-479.

593 Zhang, Y., Ma, J., Shi, L., Cao, D. and Quan, X. (2016) Joint toxicity of cadmium and
594 SDBS on *Daphnia magna* and *Danio rerio*. *Ecotoxicology* 25(10), 1703-1711.

595 Zhang, Y., Ma, J., Zhou, S. and Ma, F. (2015) Concentration-dependent toxicity effect
596 of SDBS on swimming behavior of freshwater fishes. *Environmental Toxicology and*
597 *Pharmacology* 40(1), 77-85.

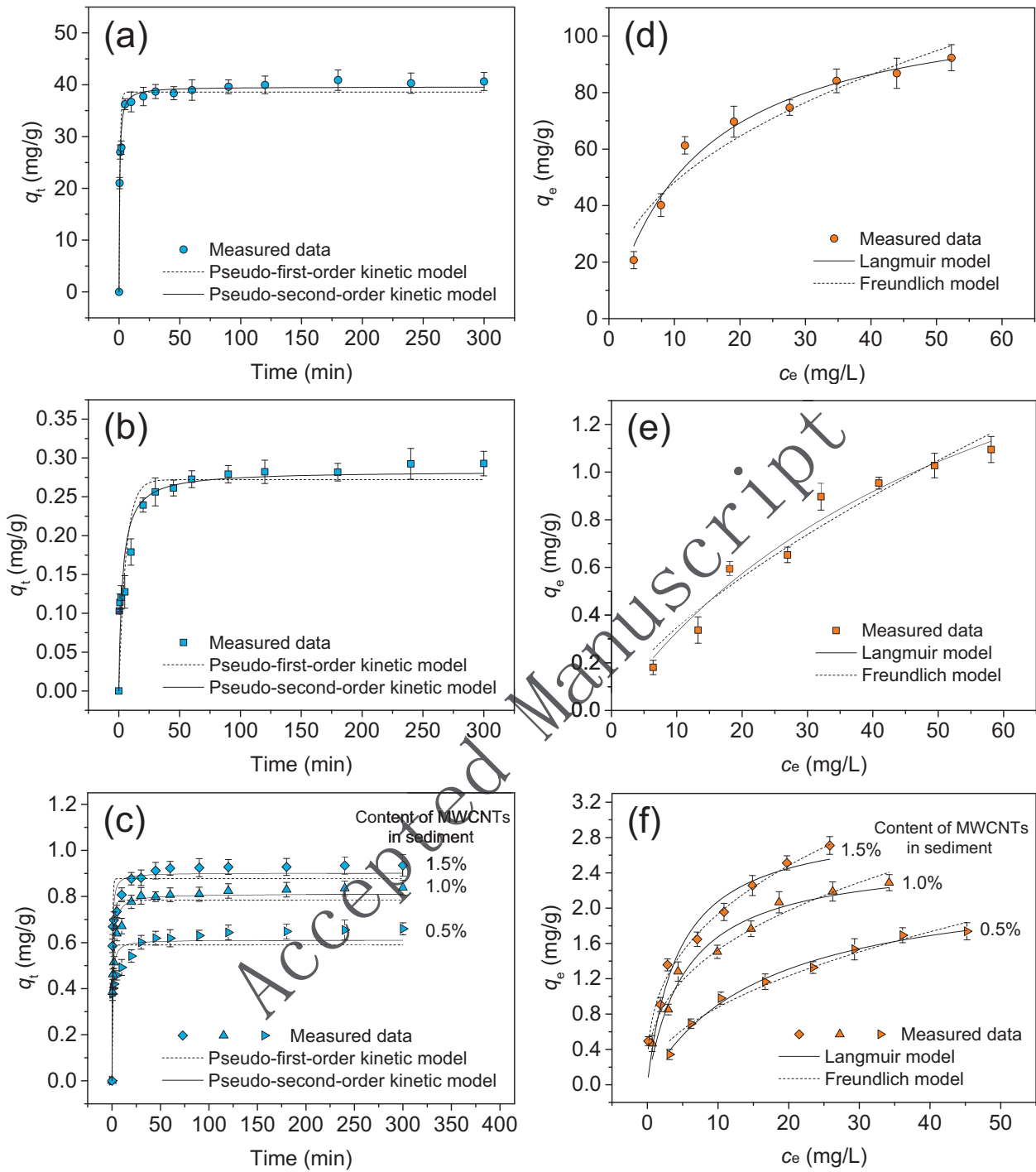
598 Zhang, Y., Zeng, G.M., Tang, L., Huang, D.L., Jiang, X.Y. and Chen, Y.N. (2007) A
599 hydroquinone biosensor using modified core-shell magnetic nanoparticles supported
600 on carbon paste electrode. *Biosensors and Bioelectronics* 22(9), 2121-2126.

601 Zhuang, J., Flury, M. and Jin, Y. (2003) Colloid-facilitated Cs transport through
602 water-saturated Hanford sediment and Ottawa sand. *Environmental Science &*
603 *Technology* 37(21), 4905-4911.

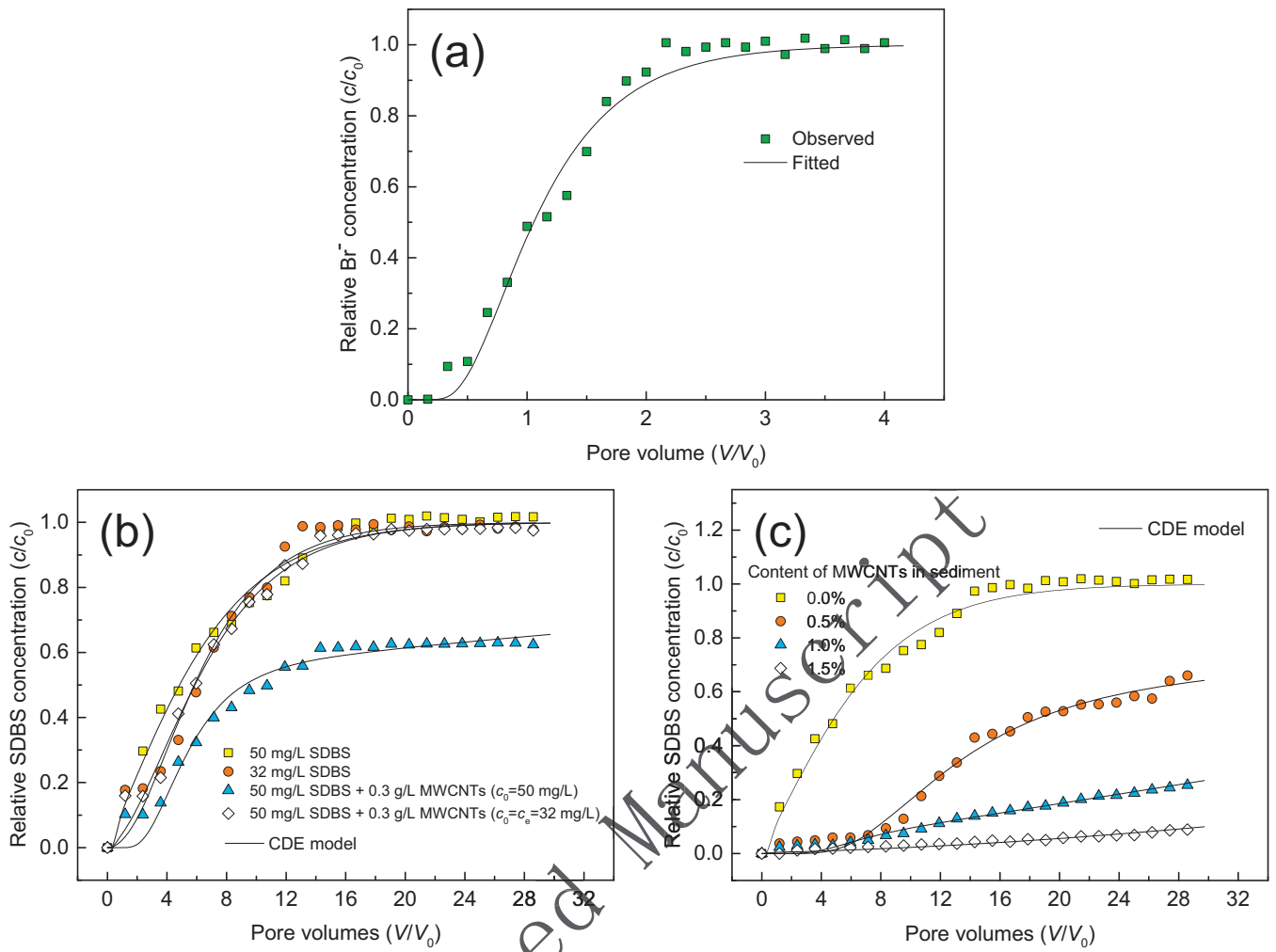
604

Accepted Manuscript

605 **Figure 1**



606 **Fig. 1.** Kinetic (a, b, and c) and isotherm (d, e, and f) studies of SDBS adsorption onto
 607 MWCNTs (a and d), sediment (b and e), and sediment-MWCNTs mixtures (c and f).
 608



610

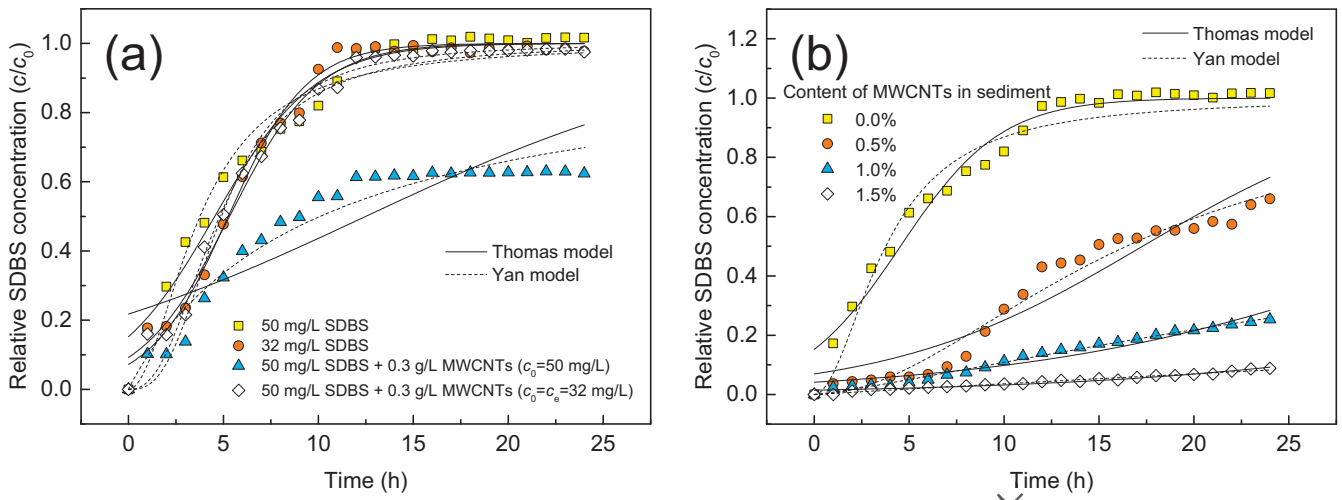
611 **Fig. 2.** Br^- breakthrough curve fitted with deterministic equilibrium CDE model (a)

612 and SDBS breakthrough curves fitted with deterministic nonequilibrium CDE model

613 (two-site chemical nonequilibrium model) for Set I (b) and Set II (c).

614

615 **Figure 3**



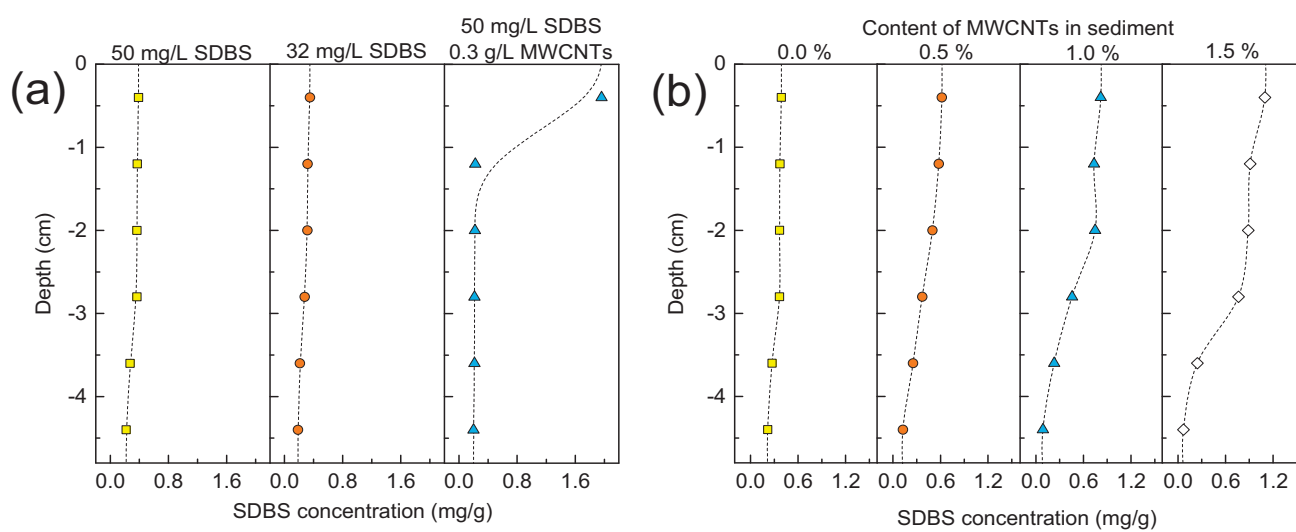
616 **Fig. 3.** SDBS breakthrough curves fitted with Thomas and Yan models for Set I (a)

617 and Set II (b).

618

Accepted Manuscript

619 **Figure 4**



620 **Fig. 4.** Retention profiles of SDBS in sediment columns for Set I (a) and Set II (b).

621

Accepted Manuscript

622 **Table 1**
 623 Parameters of the two-site chemical nonequilibrium model for fitting breakthrough curves of
 624 SDBS.

		R	β	ω	R^2
Set I	Influent				
	50 mg/L SDBS	5.10	0.196	3.12	0.981
	32 mg/L SDBS	5.62	0.178	9.53	0.977
	50 mg/L SDBS + 0.3 g/L MWCNTs ($c_0=50$ mg/L) ^a	37.0	0.155	0.646	0.966
	50 mg/L SDBS + 0.3 g/L MWCNTs ($c_0=c_e=32$ mg/L) ^b	5.78	0.173	6.22	0.989
Set II	Content of MWCNTs in sediment (% _{w/w})				
	0.0	5.10	0.196	3.12	0.981
	0.5	42.7	0.313	0.518	0.983
	1.0	60.6	0.158	3.53	0.980
	1.5	92.6	0.0108	10.3	0.927

625 ^a Using 50 mg/L as the initial concentration of SDBS for fitting the data.

626 ^b Using 32 mg/L (the equilibrium concentration) as the initial concentration of SDBS for fitting the data.

627

Accepted Manuscript

628 **Table 2**

629 Parameters of Thomas and Yan models for fitting breakthrough curves of SDBS.

		Thomas model			Yan model		
		$K_T \times 10^{-3}$ (L/h/mg)	q_T (mg/g)	R^2	$K_Y \times 10^{-3}$ (L/h/mg)	q_Y (mg/g)	R^2
Set I	Influent						
	50 mg/L SDBS	7.56	0.170	0.975	0.582	0.0730	0.962
	32 mg/L SDBS	15.2	0.126	0.992	1.32	0.0419	0.975
	50 mg/L SDBS + 0.3 g/L MWCNTs ($c_0=50$ mg/L) ^a	2.05	0.469	0.752	0.291	0.390	0.951
	50 mg/L SDBS + 0.3 g/L MWCNTs ($c_0=c_c=32$ mg/L) ^b	13.4	0.128	0.988	1.14	0.0474	0.985
Set II	Content of MWCNTs in sediment (%, w/w)						
	0.0	7.56	0.170	0.975	0.582	0.0730	0.962
	0.5	3.00	0.649	0.913	0.580	0.318	0.971
	1.0	1.84	1.28	0.933	0.360	1.81	0.992
	1.5	1.61	1.97	0.951	0.300	9.96	0.980

630 ^a Using 50 mg/L as the initial concentration of SDBS for fitting the data.

631 ^b Using 32 mg/L (the equilibrium concentration) as the initial concentration of SDBS for fitting the data.

Accepted Manuscript